Published in Electric Power Systems Research with doi: 10.1016/j.epsr.2022.108946

Multi-objective Home Energy Management Systems in nearly-Zero Energy Buildings under Uncertainties considering Vehicle-to-Home: A Novel Lexicographic-based Stochastic-Information Gap Decision Theory Approach

Marcos Tostado-Véliz[1], Hany M. Hasanien[2,*], Salah Kamel[3], Rania A. Turky[4], Francisco Jurado[1,*] and M. R. Elkadeem[5]

1. Department of Electrical Engineering, University of Jaén, Linares 23700, Spain (e-mail: mtostado@ujaen.es (M.T.-V.), fjurado@ujaen.es (F.J.))
2. Electrical Power and Machines Department, Faculty of Engineering, Ain Shams University, Cairo 11517, Egypt (e-mail: hanyhasanien@ieee.org)
3. Department of Electrical Engineering, Faculty of Energy Engineering, Aswan University, Aswan 81528, Egypt (e-mail: skamel@aswu.edu.eg)
4. Electrical Engineering Department, Faculty of Engineering and Technology, Future University in Egypt, Cairo 11835, Egypt (e-mail: rania.turky@fue.edu.eg)
5. Electrical Power and Machines Engineering Department, Faculty of Engineering, Tanta University, Tanta 31521, Egypt (e-mail: mohammad.elkadim@f-eng.tanta.edu.eg)

Correspondence (*): hanyhasanien@ieee.org, fjurado@ujaen.es

Abstract - Residential sector is being promoted to evolve towards nearly-Zero Energy Buildings (nZEBs), which draw a yearly net energy consumption near to zero. This target can be attained through on-site renewable generation with achieving a high degree of efficiency in the consumption. In this context, Home Energy Management (HEM) systems become an indispensable tool for obtaining optimally coordinating smart appliances, renewable generation and on-site storage facilities. Due to the high unpredictability of renewable generation and some emerging appliances like electric vehicles, these tools must be able to properly deal with different uncertainties while a variety of objectives are jointly considered. The existing approaches normally fail to jointly deal with these two premises. This paper aims at filling in this gap by developing a novel solution procedure for HEM systems in nZEBs. The proposed procedure is based on lexicographic optimization to find a compromise solution among objectives, while the variety of uncertainties caused by unpredictable weather, demand, energy pricing and electric vehicle behaviour are properly modelled using a hybrid stochastic-Information Gap Decision Theory (IGDT) approach. The mathematical modelling is sufficiently comprehensive (comprising various energy sources and vehicle-to-home capability) as well as it is tractable due to its integer-linear structure. A case study on a benchmark nearly zero energy home is considered to validate the developed approach which its results reveal its effectiveness in term of minimizing various objective functions, while the degree of robustness is preserved and the whole procedure is efficient yet.

Keywords: home energy management; multi-objective optimization; Nearly zero energy buildings; uncertainties; vehicle-to-home.

Nomenclature

Indices (Sets)

$s(\mathcal{S})$	scenario
$r(\mathcal{R})$	representative scenario
$t(\mathcal{T})$	time
$k(\mathcal{K}^{\mathrm{NI}}/\mathcal{K}^{\mathrm{I}})$	non-interruptible/interruptible controllable appliance
Θ	electric vehicle plugging window
Ψ	controllable appliance time window
Ω	cluster of a representative scenario

Superscripts

$Grid$	utility grid
PV	photovoltaic pannels
$Air, out/in$	outdoor/indoor air
WT	wind turbine
$BES, ch/dch$	battery energy storage in charging/discharging mode
$PEV, ch/dch$	plug-in electric vehicle in charging/discharging mode
$HVAC, h/c$	heating-ventilation-air conditioner system in heating/cooling mode
sp/db	set-point/deadband
$w, h/c$	hot/cold water
EWH	electric water heater
NC	non-controllable appliances
$\underline{(*)}/\overline{(*)}$	minimum/maximum value of a variable/parameter
$\widehat{(*)}$	uncertain parameter

Parameters

π	probability (pu)
$\Delta\tau$	time step (h)
ϑ	solar irradiance (kW/m²)
θ	temperature (ºC)
η	efficiency (pu)
γ	wind speed (m/s)
a, b	coefficients of the wind turbine power curve (kW/(m/s)³, -)
ε_0^{PEV}	initial state-of-charge of the electric vehicle (kWh)
δ	duty cycle of a controllable appliance (-)
m	mass (kg)
Q	heat or thermal capacity ($\mathrm{kJ}/(\mathrm{kg}\cdot°\mathrm{C})$ or kWh/ºC)
R	equivalent thermal resistance of the building (kW/ºC)
C	coefficient of performance (pu)
λ	energy price ($/kWh)

Functions

$\mathrm{E}(*)$	estimated value of an uncertain parameter
$\mathrm{size}(*)$	number of elements within a cluster or set

Decision variables

p	power (kW)
u	commitment status (binary)
ε	energy stored (kWh)
on/off	ON/OFF status of appliances (binary)

1 - Introduction

1.1 - Context & motivation

Electricity demand is expected to grow continuously during the following years [1]. This trend supposes a barrier to the decarbonisation of the system due to the massive dependency on fossil fuels [2]. In this context, there is a high interest on reducing energy consumption. The residential sector represents an important percentage of the total electricity consumption and greenhouse gases emissions worldwide [3]. In consequence, many organizations have put their focus on reducing domestic energy consumption. For instance, the Directive 2018/844/EU refers that by 2050 all residential and commercial existing buildings must be renovated in order to increase their energy efficiency [4]. The measures to increase energy performance in buildings are normally divided into two categories, namely energy savings and renewable energy sources (RESs) utilization [5].

The nearly-Zero Energy Buildings (nZEBs) are defined in the 2010/31/EU Directive as buildings with nearly zero primary energy consumption, meanwhile utilizing building-integrated RESs as much as possible. Particularly, photovoltaic (PV) or wind-generation (WG) units are the most frequently deployed system either on-site or near the nZEBs [3]. These assets are usually combined with storage facilities to manage the intermittent behaviour of RESs; thus increasing energy utilization and optimizing self-consumption. The emergence of smart appliances enables opportunities for further energy savings, but also increases the complexity of home installations. In this sense, the use of home energy management (HEM) systems becomes essential to effectively coordinate the operation of

RESs, on-site storage facilities and smart appliances [6]. Indeed, a recent study points out that nearly 15-40% of domestic demand can be reduced using HEM systems [7]. Besides, plug-in electric vehicles (PEVs) through vehicle-to-home (V2H) features could offer the benefit of optimizing the use of locally generated renewable energy while also providing revenue opportunities [8].

A HEM system allows to schedule of the different domestic appliances and storage assets to maximize building efficiency or economy [9]. Therefore, it must adequately handle the uncertainties raised from renewable sources or dynamic pricing tariffs such as real-time pricing (RTP) schemes [10]. In this regard, uncertainties modelling becomes a vital pillar in HEM programs, being so necessary to model not only the stochastic character of energy price and renewable generation but also the unpredictable behaviour of some emerging appliances like PEVs [11].

This paper aims to tackle the challenges described above. To this end, a new Lexicographic-based stochastic-IGDT approach for multi-objective HEM systems in n-ZEB under uncertainties with V2H operation is developed.

1.2 - Literature review

In recent years, many studies have developed different HEM approaches for nZEBs. Paterakis, et al, developed in [10] an appliance scheduling model under RTP and load-shaping strategies. The developed scheduler was formulated as a single-objective Mixed-Integer Linear Programming (MILP), considering RTP pricing and vehicle-to-home (V2H) capability. Kazmi, et al. [12] presented a data-driven scheduling approach to improve energy performance in nZEBs through the reduction in hot water consumption. In this reference, extensive simulations were performed in 46 real nZEBs, reducing the energy consumption in district hot water up to 27%. Kang [13] proposed a design

algorithm for high-efficient buildings. To this end, a statistical analysis was proposed, taking data for real cases. With the use of these data, the developed algorithm determines the best practice and calculates the lifecycle cost of the project. In [14], various metaheuristics optimizers were tested for getting the optimal appliances scheduling problem, concluding that the developed enhanced differential teaching-learning algorithm offered the best trade-off between the optimum solution and computational efficiency.

In [15], a novel HEM model was developed, which incorporates various indicators to measure the comfort and degree of acceptance of inhabitants. The proposed model considers the minimization of energy cost and users' disturbance as objectives, using a metaheuristic algorithm for solving the optimization problem. Shafie-Khah and Siano developed in [16] a stochastic-based HEM system, considering V2H and response fatigue. In this model, uncertainties from renewable generation and PEV are considered via scenarios, using a reduction technique to alleviate the computational cost of the solution procedure. Zhao, et al. [17] proposed a robust HEM system, in which the worst-case of uncertainties is extracted analytically and incorporated to obtain a robust solution of the optimization problem, which jointly considers energy cost and weariness. The genetic algorithms and cross-entropy operators are used for solving the HEM problems in [18]. In this reference, a conventional formulation of the problem is considered to minimize the energy cost.

Moreover, Heim, et al. [19] showed how the structure of the building can be exploited as thermal storage, leading to nZEB capacity by the optimal interaction of individual buildings and the main grid in energy markets. In [20], the authors explored the role of natural ventilation for energy savings in nZEBs. To this end, a sophisticated model is developed to predict air temperature while the importance of the building model is

highlighted. A self-scheduling HEM model was developed in [21] for smart homes with high PV penetration. A discomfort index is proposed to consider the disturbance of the scheduling results in users' daily routines. In [22] a comprehensive multi-objective control was developed for nZEBs for which metaheuristic algorithms were employed. The objective function was formulated to encompass energy cost, users' satisfaction and maximum exploitation of the renewable system by an optimal operation of a battery energy storage (BES) system. The authors of [23] proposed a hybrid neural network combined with genetic algorithms to optimally schedule the operation of a residential system. A similar model was built in [24], but linear optimization was executed instead of heuristic approaches.

A multi-objective MILP-based HEM system model was presented in [25] and solved using the epsilon-constraint algorithm. In [6], an advanced HEM model was developed incorporating inverter-based air conditioner devices. An optimal electrification tool for isolated homes was developed in [11] incorporating the uncertainties from renewable generation and PEV using representative days and stochastic models, using clustering techniques to reduce the scenario-space to make the optimization problem easily manageable. Mancò, et al, developed in [26] a nonlinear design-operation strategy for nZEBs, including cold and thermal loads with a wide variety of generation units and storage facilities.

Most recently, a sizing methodology for RESs and BES in nZEBs was developed in [27], which allows considering the impact of the depth-of-discharge (DOD), depreciation, ageing and fed-in rate in the total project cost. The model was comprehensively formulated taking historical data of renewable generation, which leads to a nonlinear optimization problem that is solved using metaheuristic algorithms. Ahmadiahangar, et al, proposed in [28] a heuristic algorithm to maximize self-consumption in nZEBs. The

developed approach maximizes the use of PV generation by properly scheduling a BES. The model was validated in a real case placed in the Baltic Region. In [29], a many-objective optimization procedure for HEM systems was developed to efficiently manage a six-objective optimization problem combining lexicographic optimization and scalarizing functions. The resulting problem incorporates the uncertainties from demand and renewable generation using stochastic programming and clustering techniques.

In order to provide a broad survey of the literature, a descriptive and statistical co-occurrence-based bibliometric analysis on the author's keywords is performed using VOSviewer software[1]and relying on the Scopus database[2] from 2010 and 2021. The search query was chosen to serve the primary goal of this study based on the first two keywords. The analysis results in 1270 journal articles concerning HEM or nZEBs studies and identified 94 keywords grouped in 4 clusters in different colours as visualized in Fig. 1-a. The findings specify numerous remarkable tendencies presenting in the network, which comprises multiple keywords. Obviously, the most commonly cited terms, which articles are intensely focused on, with outstanding link strength with other terms are HEM (375 occurrences, 607 link strength), nZEBs (291, 330), demand response (160, 377), and smart grid [29] (141, 348). Moreover, the proposed co-occurrence timeline visualization map illustrated in Fig. 1-b enunciates the most recent emerging topics in the vibrant research community with red colour. This includes electric vehicles, internet of things, battery energy storage, multi-objective optimization, machine learning, appliance scheduling and grid interaction, all achieving an average publication year of nearly 2019.

[1] https://www.vosviewer.com/
2 https://www.scopus.com/

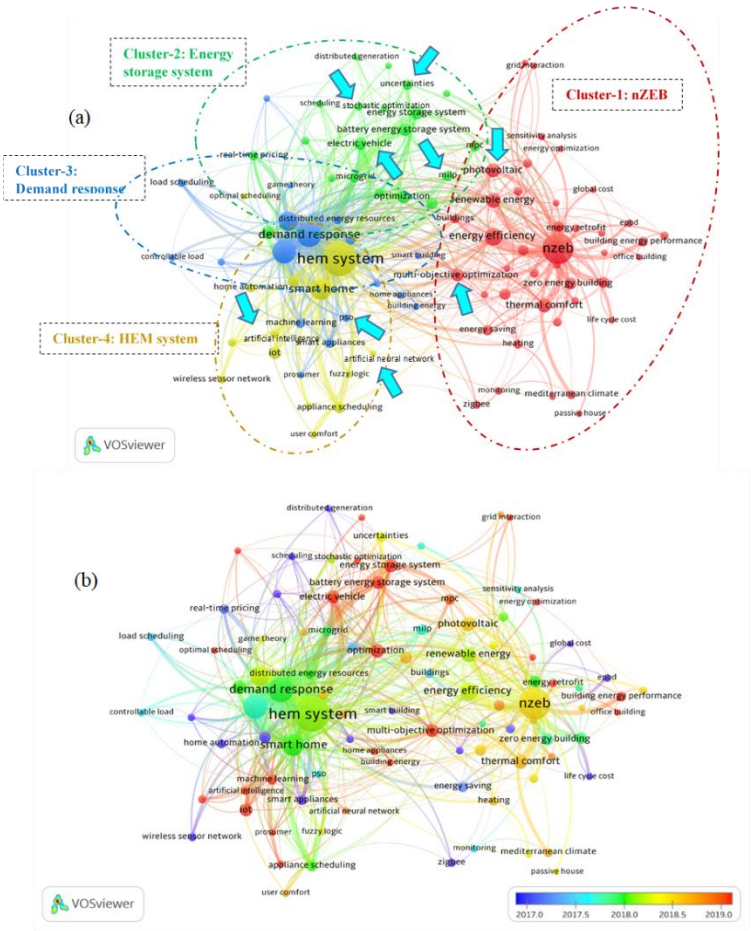

Figure 1 – Author's keywords co-occurrence analysis in the context of the investigated subject (a) Network visualization by cluster (b) Overlay visualization by average publication date. *(Note: circle size represents the number of co-occurrences of a keyword in articles, threshold number of occurrences were set to 6 times per keyword, circle color in (a) is cluster group, and color in (b) is the average publication year of articles that used a keyword)*

1.3 - Contributions & paper organization

Despite the notable importance of uncertainties modelling in HEM systems for nZEBs, there is still considerable space for further developments. Table 1 presents a summary of the studied references in terms of the solution method, objectives and uncertainties.

Table 1 - A summary of the studied references and the present work

Ref.	Formulation	Objective	RTP	PV	WG	V2H	Uncertainties
[10]	MILP	Single	Yes	Yes	No	Yes	No
[12, 18]	Metaheuristic	Single	No	Yes	No	No	No
[13]	Heuristic	Single	No	Yes	No	No	No
[14]	Metaheuristic	Weighted-sum	Yes	Yes	No	No	No
[15]	Metaheuristic	Weighted-sum	Yes	Yes	No	Yes	No
[16]	MILP	Single	Yes	Yes	No	Yes	Stochastic
[17]	Nonlinear	Weighted-sum	No	Yes	No	No	Robust
[19]	MILP	Single	Yes	Yes	No	No	No
[21, 6]	MILP	Weighted-sum	Yes	Yes	No	No	Stochastic
[22]	Metaheuristic	Weighted-sum	Yes	Yes	Yes	No	No
[23]	Metaheuristic	Weighted-sum	No	Yes	No	No	No
[24]	MILP	Weighted-sum	No	Yes	No	No	No
[25]	MILP	Epsilon-constraint	Yes	Yes	No	No	Stochastic
[11]	MILP	Single	No	Yes	No	Yes	Stochastic
[26]	Nonlinear	Single	No	Yes	Yes	No	No
[27]	Metaheuristic	Single	No	Yes	Yes	No	No
[29]	Heuristic	Single	No	Yes	No	No	No
[30]	MILP	Lexicographic-Scalarizing	No	Yes	No	No	Stochastic
Present	MILP	Lexicographic	Yes	Yes	Yes	Yes	Hybrid

In the light of the above bibliometric analysis and data summarized in Table 1, the following gaps have been detected.

- Most of the literature **ignores the effect of uncertainties** in the energy management of nZEBs *(see Fig. 1, the term uncertainties is repeated only 19 times and has weak link strength of 5 with nZEB terms)*. In such cases, it is frequently assumed that forecast profiles are deterministic [10]. In other cases, simple stochastic formulations are proposed [16]. This approach is simple and reliable; however, it may be unsuitable for certain parameters such as those related to PEVs.
- The majority of the existing HEM models **do not consider some important components and capabilities**. This is the case of V2H and WG, which are usually ignored [12, 18]. In contrast, most of the researchers consider only PV units [14] (*reveal Fig. 1, PV has 40 occurrences and 11 link strength of 12 with HEM and 11 with nZEB*).
- In most cases, two or more objective functions are involved [30] while addressing the domestic energy management problems (*see Fig. 1, the term multi-objective*

has relatively high occurrences (29), and a strong link strength with other terms (57)). In the literature, **the weighted sum is typically considered for solving such multi-objective HEM problems**. This approach, however, has two critical drawbacks: (i) the obtained solution is strongly impacted by the value of the weights, which are frequently heuristically fixed and (ii) it is difficult to handle the objective of different units and, moreover, the resulting Pareto fronts present a low density of solutions [31].

- Frequently, the formulation of the optimization problem is nonlinear, being so necessary to **use heuristic or metaheuristic solvers,** particularly PSO algorithm (*refer Fig. 1*). But these techniques may be trapped on local optimums as well as present a no-modular structure. In this sense, **MILP formulations are by far preferred** [10] *(see Fig. 1, the terms MILP has been repeated 18 times and attained a value of 29 as a total link strength with other terms such as HEM system, nZEB smart home, and demand response).*

This paper aims at addressing the gaps exposed above. Consequently, a novel HEM system suitable for nZEBs is developed. The new proposal combines stochastic programming with Information Gap Decision Theory (IGDT). This approach is based on the different character of the uncertainties involved, as already proposed for other related problems [32, 33]. Indeed, whereas weather and demand uncertainties can be easily modelled via scenarios since their probabilities or predicted errors can be modelled by distribution functions [34], the unpredictable behaviour of PEVs should be handled differently. In this sense, the proposed model based on IGDT features the ability to predict the worst-case values of the uncertainties raised with PEV. The main contributions of this paper are enumerated as:

- A novel HEM model for nZEBs is developed, which presents a modular MILP formulation which can be efficiently managed by conventional solvers and machines.
- A novel hybrid scheme is proposed with the aim of managing the uncertainties. This scheme combines the conventional stochastic optimization to handle uncertainties from weather, energy price and demand, whereas IGDT is employed to model the unpredictable behaviour of PEVs.
- In contrast to other works, RTP [10], V2H [11] and WG are properly modelled in the home system, in order to consider all the possibilities and capabilities of nZEBs.
- A modular bi-objective structure is presented to optimize the energy consumption and cost. To this end, a novel lexicographic scheme is developed, which serves as a suitable framework to incorporate uncertainties using IGDT. Due to its modular structure, the multi-objective solution procedure presented in this paper can easily accommodate more uncertainties.

Resulting from the contributions above, the present work circumvents the major issues encountered in the literature, as shown in Table 1. The developed HEM model is validated using a benchmark grid-connected nZEBs supplied by PV and WG units. The considered case study encompasses a BES and a variety of controllable loads along with a charging point for PEVs to illustrate how the uncertainties of the electric vehicle are modelled and treated.

In the rest of this paper, Section 2 overviews the nZEB layout under study. Section 3 presents the mathematical models of the different appliances and on-site assets. Section 4 presents the developed HEM solution procedure. Section 5 presents a case study and the obtained results. Finally, the main conclusions are duly drawn in Section 6.

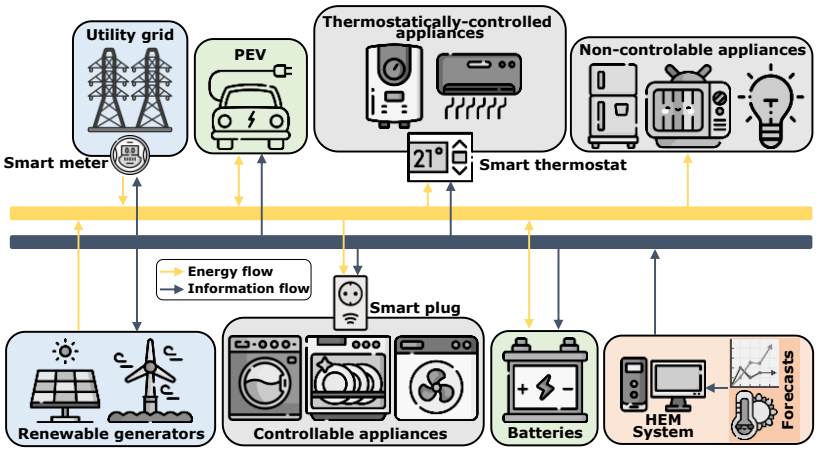

Figure 2 - Pictorial representation of the nZEB under study

2 - Overview of the nZEB under study

Fig. 2 pictorially represents the home system under study. The different appliances and on-site assets are controlled in a centralized fashion by the HEM system, which performs the scheduling plan of the different controllable devices with day-ahead periodicity. To this end, it is assumed that the forecast information of various uncertain parameters is available with sufficient accurateness, which is a plausible assumption nowadays even when using conventional forecast techniques [35]. With this information, the HEM system can send scheduling and set-point signals to the different assets.

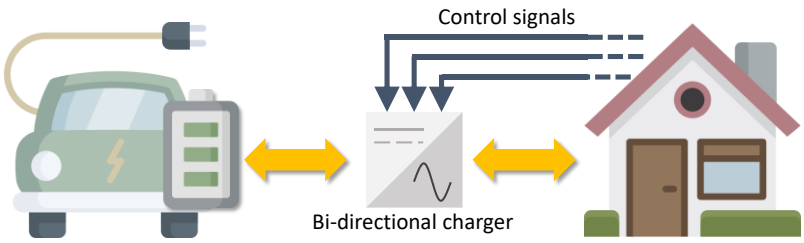

Figure 3 - Illustrative description of the V2H capability of the PEV

The building can purchase energy from the utility grid and it is also supplied employing on-site renewable generators. The imported energy has a cost per kWh imposed by the local utility. In this paper, an RTP pricing mechanism is assumed for the energy bought from the grid, nevertheless, other well-known mechanisms like the time-of-use tariffs could be considered. A storage facility formed by batteries allows to efficiently manage eventual surplus renewable energy. The storage assets can be also exploited to improve the economy of the system, thus buying energy during off-peak hours to be posteriorly consumed when the energy pricing is expected to be high (peak hours) [36]. The PEV can be also operated as a storage facility thus taking advantage of its V2H capability. To this end, it is assumed that the PEV is connected to the home through a bidirectional charger, as shown in Fig. 3, which allows bidirectional power flows (from and to the PEV). In contrast to the BES, the PEV can be only scheduled when it is plugged, bringing therefore additional uncertainties (initial state-of-charge (SOC) and departure time) [16].

Finally, domestic appliances are classified into controllable and non-controllable [21]. The non-controllable appliances are assumed to be scheduled under human decisions. This way, they are inhibited of the HEM operation. Nevertheless, since their consumption patterns usually respond to daily routines, their demand can be predicted with acceptable accurateness [21, 30]. In contrast, smart plugs enable active control of some appliances directly from the HEM system. This kind of controllable appliances may be scheduled within predefined time windows, which are assumed to be set by the users on the basis of their preferences [25]. The controllable appliances are in turn classified into interruptible and non-interruptible. In the former case, their operation can be interrupted without disturbing their functionality, whereas the non-interruptible appliances cannot be shut down until completing their duty cycle [30]. Lastly, the thermostatically controlled

appliances are operated through smart thermostats, which continuously control the indoor and hot water temperatures, in the case of the heating-ventilation-air conditioner (HVAC) system and electric water heater (EWH), respectively. This way, the operation of the thermostatically controlled appliances can be scheduled and their consumption is continuously controlled in order to maintain the thermal comfort of the inhabitants within acceptable bounds [30].

3 - Mathematical models

In this section, the mathematical modelling of the different devices described in Section 2 is presented. The subsequent formulation is then incorporated into the optimization problem as operating constraints. The different mathematical models are developed over the representative scenario-space ($\mathcal{R}$), since some of the uncertainties are modelled using stochastic programming (see Section 4).

3.1 - Connection to the utility grid

The home system under study can purchase energy from a utility grid, which is owned by the local service entity [10]. It is realistic to assume that imported power is actually bounded by contractual conditions or physical limits [9, 30], as said the constraint (1).

$$p_{r|t}^{Grid} \leq u_{r|t}^{Grid} \cdot \bar{p}^{Grid};\ \forall r \in \mathcal{R} \wedge t \in \mathcal{T} \tag{1}$$

3.2 - PV modelling

Potential PV generation is strongly influenced by weather parameters such as temperature and solar irradiation [37]. In this paper, the model developed in [38] is considered, which calculates the instantaneous PV potential, as follows

$$\phi_{\mathrm{r|t}}^{\mathrm{PV}} = \overline{\mathrm{p}}^{\mathrm{PV}} \cdot \left[0.25 \cdot \hat{\vartheta}_{\mathrm{r|t}} + 0.03 \cdot \hat{\vartheta}_{\mathrm{r|t}} \cdot \hat{\theta}_{\mathrm{r|t}}^{\mathrm{Air,out}} + (1.01 - 1.13 \cdot \eta^{\mathrm{PV}}) \cdot \hat{\vartheta}_{\mathrm{r|t}}^{2}\right];\ \forall r \in \mathcal{R} \wedge t \in \mathcal{T} \tag{2}$$

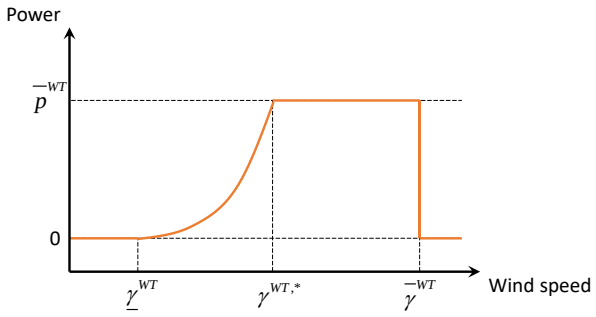

Figure 3 - A typical wind speed curve for a wind turbine

As observed, the temperature and solar irradiance are considered uncertain parameters in (2), for which proper models are described in Section 4. As pointed out in [9, 30], additional constraints should be imposed to limit the power extracted from PV panels. This is because the expression (2) may eventually yield values higher than $\overline{p}^{PV}$, which is not a realistic assumption since typically inverters limit the power generated to avoid failure of components. To solve this issue, constraint (3) has to be imposed.

$$p_{r|t}^{PV} \leq \begin{cases} \phi_{r|t}^{PV}, & \text{if } \phi_{r|t}^{PV} \leq 1.1 \cdot \overline{p}^{PV} \\ \overline{p}^{PV}, & \text{otherwise} \end{cases} ; \forall r \in \mathcal{R} \wedge t \in \mathcal{T} \quad (3)$$

In (3), it is assumed that 10% overloads are allowed, which is a plausible assumption in real cases [30].

3.3 - WG modelling

In the case of wind turbines, the available wind generation is directly related to the wind speed and can be calculated by the well-known wind-power curve of a wind turbine [40]. Fig. 3 plots a typical wind power curve which is defined by maximum and minimum speed values and the parameter $\gamma^{WT,*}$, which indicates the value of the wind speed beyond which the turbine produces its rated power.

Mathematically, the curve plotted in Fig. 3 can be easily modelled by its piecewise representation [41], splitting it into four sections, as said (4) [42], while the constraint (5)

considers the efficiency of the turbine components. As seen, the expression (4) considers the wind speed an uncertain parameter.

$$\phi_{r|t}^{WT} = \begin{cases} 0, & if\ \hat{\gamma}_{r|t} < \underline{\gamma}^{WT} \\ a \cdot \hat{\gamma}_{r|t}^{3} - b \cdot \bar{p}^{WT}, & \text{if } \underline{\gamma}^{WT} \le \hat{\gamma}_{r|t} < \gamma^{WT,*} \\ \bar{p}^{WT}, & \text{if } \gamma^{WT,*} \le \hat{\gamma}_{r|t} < \bar{\gamma}^{WT} \\ 0, & if\ \hat{\gamma}_{r|t} \ge \bar{\gamma}^{WT} \end{cases}; \ \forall r \in \mathcal{R} \wedge t \in \mathcal{T} \tag{4}$$

$$p_{r|t}^{WT} \le \eta^{WT} \cdot \phi_{r|t}^{WT};\ \forall r \in \mathcal{R} \wedge t \in \mathcal{T} \tag{5}$$

3.5 - BES modelling

In the case of batteries, the maximum power that can exchange with the installation is limited by rated values [6, 10], as ensured by the constraint (6). On the other hand, (7) is applied to avoid the simultaneous charging and discharging of the BES.

$$p_{r|t}^{BES,i} \le u_{r|t}^{BES,i} \cdot \bar{p}^{BES};\ \forall r \in \mathcal{R} \wedge t \in \mathcal{T} \wedge i \in \{ch, dch\} \tag{6}$$

$$u_{r|t}^{BES,ch} + u_{r|t}^{BES,dch} \le 1;\ \forall r \in \mathcal{R} \wedge t \in \mathcal{T} \tag{7}$$

Further, equation (8) models the SOC of the batteries [30], which is limited by their nominal capacity and depth-of-discharge (DOD) settings, as expressed by (9).

$$\varepsilon_{r|t}^{BES} = \varepsilon_{r|t-1}^{BES} + \Delta\tau \cdot \left(\eta^{BES} \cdot p_{r|t}^{BES,ch} - {p_{r|t}^{BES,dch}}\Big/{\eta^{BES}} \right);\ \forall r \in \mathcal{R} \wedge t \in \mathcal{T} \backslash t > 1 \tag{8}$$

$$\underline{\varepsilon}^{BES} \le \varepsilon_{r|t}^{BES} \le \bar{\varepsilon}^{BES};\ \forall r \in \mathcal{R} \wedge t \in \mathcal{T} \tag{9}$$

For adequate and accurate BES modelling, it is necessary to define the initial SOC of the batteries. Similar to other references [30, 39], it is assumed that the BES is fully charged at the beginning of the time horizon. To keep the model coherent, the constraint (10) ensures that the initial and final SOC are equal.

$$\varepsilon_{r|\mathcal{T}(1)}^{BES} = \varepsilon_{r|\mathcal{T}(\text{end})}^{BES} = \bar{\varepsilon}^{BES};\ \forall r \in \mathcal{R} \tag{10}$$

3.6 - PEV modelling

Similar to stationary batteries, charging-discharging capabilities of the PEV are enabled through V2H capacbility. This way, equations (11)-(14) are equivalent to (6)-(9) but adapted to the PEV [11].

$$p_{r|t}^{PEV,i} \leq u_{r|t}^{PEV,i} \cdot \bar{p}^{PEV};\ \forall r \in \mathcal{R} \wedge t \in \mathcal{T} \wedge i \in \{ch, dch\} \tag{11}$$

$$u_{r|t}^{PEV,ch} + u_{r|t}^{PEV,dch} \leq 1;\ \forall r \in \mathcal{R} \wedge t \in \mathcal{T} \tag{12}$$

$$\varepsilon_{r|t}^{PEV} = \varepsilon_{r|t-1}^{PEV} + \Delta\tau \cdot \left(\eta^{PEV} \cdot p_{r|t}^{PEV,ch} - {p_{r|t}^{PEV,dch}}\Big/{\eta^{PEV}}\right);\ \forall r \in \mathcal{R} \wedge t \in \mathcal{T} \backslash t > 1 \tag{13}$$

$$\underline{\varepsilon}^{PEV} \leq \varepsilon_{r|t}^{PEV} \leq \bar{\varepsilon}^{PEV};\ \forall r \in \mathcal{R} \wedge t \in \mathcal{T} \tag{14}$$

In contrast to stationary batteries, the PEV cannot be scheduled when it is not plugged. To ensure proper scheduling of the vehicle, (15) forces its scheduling status to be zero when it is not plugged at home.

$$u_{r|t}^{PEV,ch} + u_{r|t}^{PEV,dch} = 0;\ \forall r \in \mathcal{R} \wedge t \notin \widehat{\Theta} \tag{15}$$

It is assumed that the PEV needs to be fully charged at its departure time, as declared in (16). On the other hand, (17) sets the initial SOC of the PEV. In this paper, it is assumed that the PEV can be scheduled at the beginning of the time horizon [30], which means, its arrival time occurs at $t = 1$.

$$\varepsilon_{r|\widehat{\Theta}(\text{end})}^{PEV} = \bar{\varepsilon}^{PEV};\ \forall r \in \mathcal{R} \tag{16}$$

$$\varepsilon_{r|\widehat{\Theta}(1)}^{PEV} = \hat{\varepsilon}_0^{PEV};\ \forall r \in \mathcal{R} \tag{17}$$

It is noteworthy that the PEV scheduling involves two uncertain parameters. On the one hand, the initial SOC is considered unknown since it depends on the daily mileage [43]. On the other hand, its departure time is a priori unpredictable, being possible to leave the home at any time instant. In (15)-(17), the PEV time window (Θ) is modelled as an uncertain variable to take into account this particularity.

3.7 - Controllable appliances modelling

As customary, the controllable appliances are classified into interruptible or non-interruptible [30]. In both cases, their duty cycles must be completed within the predefined time windows, as ensured (18), being not possible to schedule them out of their respective time windows, as forced by (19).

$$\sum_{t\in\Psi^k}\left\{u_{r|t}^k\right\}=\delta^k;\ \forall r\in\mathcal{R}\wedge k\in\{\mathcal{K}^{\mathrm{NI}}\cup\mathcal{K}^{\mathrm{I}}\} \tag{18}$$

$$\sum_{t\notin\Psi^k}\left\{u_{r|t}^k\right\}=0;\ \forall r\in\mathcal{R}\wedge k\in\{\mathcal{K}^{\mathrm{NI}}\cup\mathcal{K}^{\mathrm{I}}\} \tag{19}$$

The non-interruptible appliances cannot be shut down once their operating cycles have begun. To properly model this behaviour, (20) imposes continuity in their operation while (21) forces to schedule these appliances only once throughout the time horizon.

$$on_{r|t}^k-off_{r|t}^k=u_{r|t}^k-u_{r|t-1}^k;\ \forall r\in\mathcal{R}\wedge t\in\mathcal{T}\backslash t>1\wedge k\in\mathcal{K}^{\mathrm{NI}} \tag{20}$$

$$\sum_{t\in\Psi^k}\left\{on_{r|t}^k\right\}=1;\ \forall r\in\mathcal{R}\wedge k\in\mathcal{K}^{\mathrm{NI}} \tag{21}$$

3.8 - HVAC modelling

This paper adopts a resistance-based model of the building to determine the indoor temperature at any time instant. This model is based on differential equations which can be linearized [10]. In this way, the indoor temperature is calculated by (22) as a function of the outdoor temperature, the thermal resistance of the building and the action of the HVAC.

$$\begin{aligned}\theta_{r|t}^{Air,in}=&\left(1-\frac{\Delta\tau}{10^3\cdot m^{Air,in}\cdot Q^{Air,in}\cdot R}\right)\cdot\theta_{r|t-1}^{Air,in}\\&+\frac{1}{10^3\cdot m^{Air,in}\cdot Q^{Air,in}\cdot R}\cdot\theta_{r|t-1}^{Air,out}\\&+\frac{\left(p_{r|t-1}^{HVAC,h}-p_{r|t-1}^{HVAC,c}\right)}{0.000277\cdot m^{Air,in}\cdot Q^{Air,in}}\cdot C^{HVAC};\ \forall r\\&\in\mathcal{R}\wedge t\in\mathcal{T}\backslash t>1\end{aligned} \tag{22}$$

Similar to batteries, the initial and final temperatures must be fixed to keep the model tractable and coherent. In this work, it is assumed that the initial and final indoor temperatures are equal to the set-point settings of the HVAC system, as given by constraint (23).

$$\theta_{r|\mathcal{T}(1)}^{Air,in} = \theta_{r|\mathcal{T}(\text{end})}^{Air,in} = \theta^{HVAC,sp}; \forall r \in \mathcal{R} \tag{23}$$

To avoid the continuous operation of the HVAC unit, it is common to allow the indoor temperature to vary within acceptable dead-bands [30]. Thereby, the limits of the temperature are imposed by (24).

$$\theta^{HVAC,sp} - \theta^{HVAC,db} \leq \theta_{r|t}^{Air,in} \leq \theta^{HVAC,sp} + \theta^{HVAC,db}; \forall r \in \mathcal{R} \wedge t \in \mathcal{T} \tag{24}$$

Lastly, (25) is adopted to define the upper bounds of the power which can be consumed by the HVAC set to rating values, whereas (26) imposes complementarity on the heating and cooling modes of the HVAC system.

$$p_{r|t}^{HVAC,i} \leq u_{r|t}^{HVAC,i} \cdot \overline{p}^{HVAC};\ \forall r \in \mathcal{R} \wedge t \in \mathcal{T} \wedge i \in \{h, c\} \tag{25}$$

$$u_{r|t}^{HVAC,h} + u_{r|t}^{HVAC,c} \leq 1;\ \forall r \in \mathcal{R} \wedge t \in \mathcal{T} \tag{26}$$

3.9 - EWH modelling

The EWH can be easily modelled by linearized differential equations. In contrast to the HVAC system [44]. It is assumed that when hot water is drawn from the EWH, then it is completely replenished with cold water. Also, it is considered that the heater is installed inside the building. Under these assumptions, the water temperature inside the tank can be calculated by (27) and (28), depending on if the instantaneous water consumption is zero or not.

$$\theta_{r|t+1}^{w,h} = \theta_{r|t}^{w,h} + p_{r|t}^{EWH} \cdot \eta^{EWH} \cdot C^{w,h} - \left(\theta_{r|t}^{Air,in} - \theta_{r|t}^{w,h}\right) e^{\left(\frac{-\Delta\tau}{R^{w,h} \cdot C^{w,h}}\right)};\ \forall r \in \mathcal{R} \wedge t \in \mathcal{T} \backslash t < \mathcal{T} \wedge \hat{v}_{r|t}^{w,h} = 0 \quad (27)$$

$$\theta_{r|t+1}^{w,h} = \frac{\theta_{r|t}^{w,h} \cdot \left(\overline{v}^{EWH} - \hat{v}_{r|t}^{w,h}\right) + \theta_{r|t}^{w,c} \cdot \hat{v}_{r|t}^{w,h}}{\overline{v}^{EWH}};\ \forall r \in \mathcal{R} \wedge t \in \mathcal{T} \backslash t < \mathcal{T} \wedge \hat{v}_{r|t}^{w,h} > 0 \quad (28)$$

It is worth noting that the hot water consumption is considered unknown in (27) and (28). The hot water temperature must be maintained within acceptable limits, as shown in (29). In this case, the upper limit is imposed for security reasons [10, 39] while the lower one is set by the users on the basis of comfort requirements.

$$\underline{\theta}^{EWH} \leq \theta_{r|t}^{w,h} \leq \overline{\theta}^{EWH};\ \forall r \in \mathcal{R} \wedge t \in \mathcal{T} \quad (29)$$

As in the case of the indoor temperature, initial and final values for the hot water temperature must be given by the constraint (30). Lastly, the EWH modelling is completed by the constraint (31), which upper bounds the power consumption of the heater.

$$\theta_{r|\mathcal{T}(1)}^{w,h} = \theta_{r|\mathcal{T}(\text{end})}^{w,h} = \theta^{EWH,sp};\ \forall r \in \mathcal{R} \quad (30)$$

$$p_{r|t}^{EWH} \leq \overline{p}^{\text{EWH}};\ \forall r \in \mathcal{R} \wedge t \in \mathcal{T} \quad (31)$$

3.10 - Home power balance

The mathematical modelling of the proposed nZEB is completed by the constraint (32), by which the generation-load balance is ensured. As seen in (32), the instantaneous consumption attributable to non-controllable loads is considered an uncertain parameter.

$$p_{r|t}^{Grid} + p_{r|t}^{BES,dch} + p_{r|t}^{PEV,dch} + p_{r|t}^{PV} + p_{r|t}^{WT} = \hat{p}_{r|t}^{NC} + p_{r|t}^{BES,ch} + p_{r|t}^{PEV,ch} + p_{r|t}^{EWH} + \sum_{i \in \{h,c\}} \left\{p_{r|t}^{HVAC,i}\right\} + \sum_{k \in \{\mathcal{K}^{\text{NI}} \cup \mathcal{K}^{\text{I}}\}} \left\{u_{r|t}^{k} \cdot \overline{p}^{k}\right\};\ \forall r \in \mathcal{R} \wedge t \in \mathcal{T} \quad (32)$$

4 - The developed solution procedure

In the operation of nZEBs, weather parameters (i.e. temperature, solar irradiation and wind speed), non-controllable appliances demand, hot water consumption, initial SOC of the PEV and its departure time are considered uncertain parameters. In addition, the energy pricing is also considered unknown since an RTP tariff mechanism has been adopted. To properly model the different uncertainties, a novel hybrid stochastic-IGDT solution procedure is developed. In addition, the novel proposal allows for the consideration of different objective functions within a lexicographic optimization scheme.

The reason behind of this adoption is the heterogeneity of the uncertainties involved, which requires the use of different models. This way, weather parameters, demand and energy pricing can be easily forecasted and therefore their errors can be modelled using Gaussian distributions and stochastic programming [45]. Also, their probability models can be easily inferred from the literature or historical data. However, the behaviour of the PEV is hardly predictable [43] and therefore its distribution function is normally unknown. In this sense, it is more suitable to use IGDT for modelling the uncertainties referred to PEV rather than using scenarios. In this manner, the developed solution procedure yields a robust scheduling result with immunity against the PEV behaviour.

Fig. 4 is a flowchart of the developed methodology. It is composed of various stages. The **first stage** is devoted on optimizing the different objective functions using lexicographic optimization [46]. By this technique, the different objectives are sequentially optimized, thus giving different importance to each one (see [25, 30] for further details). In this paper, the energy cost and net energy consumption are jointly optimized, giving them the same importance. However, the developed procedure presents

a modular structure, being possible to incorporate other objectives. Therefore, stages 1.1 and 1.2 are devoted to calculate the lowest values (utopia points [25]) of these objectives by optimizing them separately. The **second stage** performs similar but, in this case, the PEV-related uncertainties are minimized. Although these particular parameters are not actually optimized, their minimum feasible values are necessary for the third stage. These pessimistic points yield the worst-case scenario for the initial SOC and departure time by minimizing them separately. Finally, the **third stage** performs the robust optimization of the scheduling problem. To this end, information on the lowest and highest values of the different objectives and PEV uncertainties need to be given. These data can be calculated from the previous stages. Thereby, this stage is focused on maximizing the uncertain radiuses using IGDT [47], while the different objectives are minimized at once. Hence, the developed methodology attains the best compromise solution among objectives considering immunity against the PEV uncertainties.

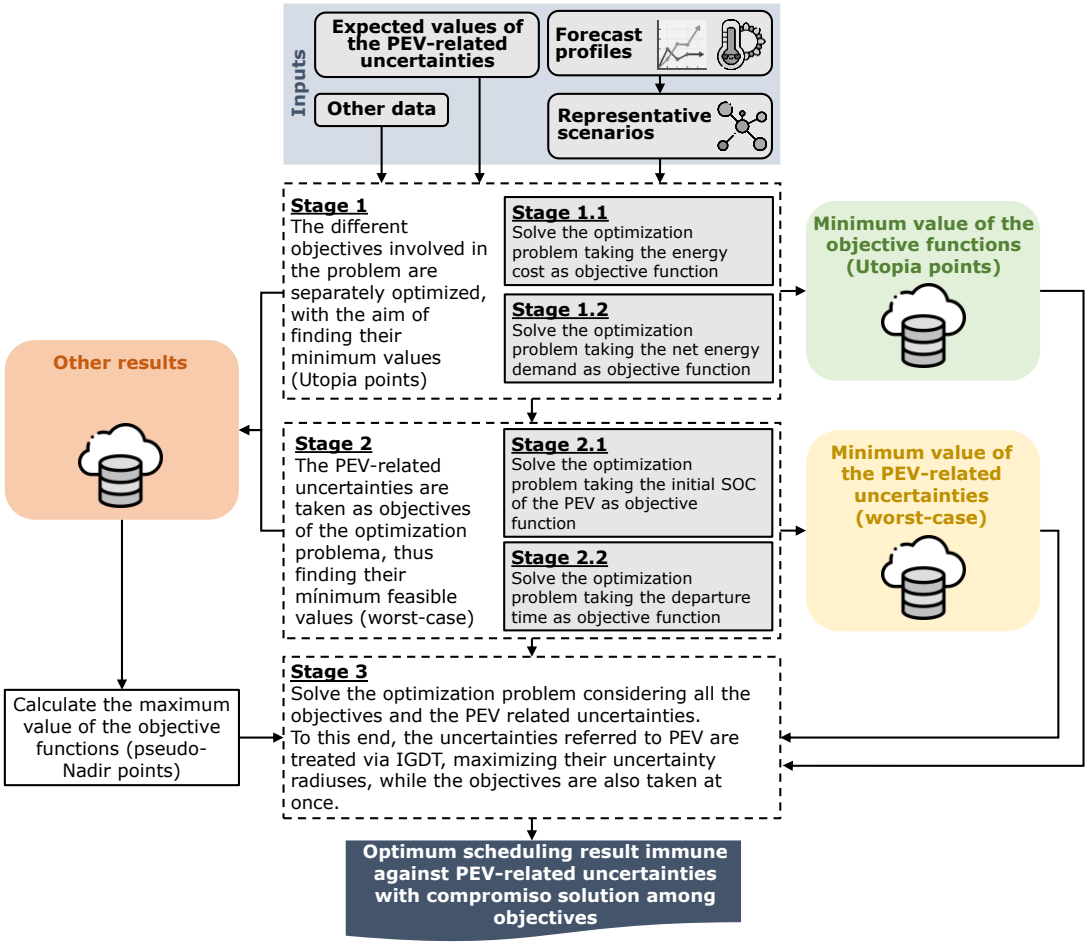

Figure 4 - Flowchart of the developed methodology

4.1 - Stochastic modelling

As commented, wind speed, energy pricing, non-controllable appliances and hot water demand, temperature and solar irradiation are modelled using stochastic programming. This approach is particularly suitable as the distribution functions of the considered uncertainties are normally well-described or their forecast errors can be modelled using Gaussian distributions [45]. In this case, the second option has been considered, which is depicted in Fig. 5. By this approach, it is assumed that the forecast profiles present precision errors which can be modelled using normal distributions [45]. Under this assumption, a large number of scenarios should be generated to effectively catch the stochastic behaviour of the concerned variable [34]. Because many scenarios have to be generated (~1,000), the resulting computational burden may be unaffordable.

Thereby, some references recur to clustering techniques intending to reduce the original scenario-space to a representative group with a smaller size, in which only some representative members from the original set are considered. In this paper, the methodology described in [48], has been considered to this end, which uses the k-medoids method and some helpful indicators for determining the members and size of the representative scenario-space. As commented in this reference, one of the main advantages of using the k-medoids method is the possibility of calculating the probability of each scenario, as follows

$$\pi_r = \frac{\text{size}(\Omega_r)}{\text{size}(\mathcal{S})};\ \forall r \in \mathcal{R} \tag{33}$$

4.2 - Stage 1

At the first stage, the different objectives involved are separately minimized considering stochastic modelling of the uncertainties explained in Section 4.1. In this regard, this stage aims at calculating the lowest values of the different objectives (utopia points). In this paper, without loss of generality, two objectives are considered, the energy cost and the net energy consumed, which can be respectively formulated as follows:

$$f_1 = \sum_{r\in\mathcal{R}} \left\{ \pi_r \cdot \sum_{t\in\mathcal{T}} \left\{ \Delta\tau \cdot \hat{\lambda}_{r|t} \cdot p_{r|t}^{Grid} \right\} \right\} \tag{34}$$

$$f_2 = \sum_{r\in\mathcal{R}} \left\{ \pi_r \cdot \sum_{t\in\mathcal{T}} \left\{ \Delta\tau \cdot \left(\begin{array}{c} \hat{p}_{r|t}^{NC} + p_{r|t}^{BES,ch} + p_{r|t}^{PEV,ch} \\ +p_{r|t}^{EWH} + \sum_{i\in\{h,c\}} \left\{ p_{r|t}^{HVAC,i} \right\} + \sum_{k\in\{\mathcal{K}^{\mathrm{NI}}\cup\mathcal{K}^{\mathrm{I}}\}} \left\{ u_{r|t}^{k} \cdot \overline{p}^{k} \right\} \\ -p_{r|t}^{BES,dch} - p_{r|t}^{PEV,dch} - p_{r|t}^{PV} - p_{r|t}^{WT} \end{array} \right) \right\} \right\} \tag{35}$$

For simplicity in the explanation, the Stage 1 is divided into the stages 1.1 and 1.2 depending on if the minimization is performed on (34) and (35), respectively. Therefore, the optimization problems for the stages 1.1 and 1.2 is stated as:

$$\underline{f_1} = f_1^{(1.1)} \rightarrow \underset{\boldsymbol{x}}{\operatorname{argmin}} f_1\left(\mathrm{E}(\Theta), \mathrm{E}(\varepsilon_0^{PEV})\right) \tag{36}$$

s.t. (1)-(32)

$$\underline{f_2} = f_2^{(1.2)} \rightarrow \underset{\boldsymbol{x}}{\operatorname{argmin}} f_2\left(\mathrm{E}(\Theta), \mathrm{E}(\varepsilon_0^{PEV})\right) \tag{37}$$

s.t. (1)-(32)

where, the superscripts $(x.x)$ indicate the value of the objective of this particular stage (e.g. $f_1^{(1.1)}$ is the value of f_1 at the stage 1.1). It is important to note that expected values of the uncertainties related to PEV are taken on the problems (36) and (37). Therefore, the Stage 1 neglects the unpredictable behaviour of the vehicle, considering its variables as deterministic. It is also important to note that other objectives could be integrated into the developed framework without any problem.

4.3 - Stage 2

The Stage 2 performs similar to the previous stage, however, this step searches the minimum value of the uncertainties referred to the PEV, i.e. the initial SOC and the departure time. It is important to note that the minimum feasible value of these parameters supposes the worst-case scenario. Therefore, to find the limit cases for which the scheduling plan is still feasible, the initial SOC and the time window Θ. In the cases of the initial energy stored in the on-board batteries, its lowest value can be easily found by declaring it as a variable, leading to the following optimization problem.

$$f_3 = \varepsilon_0^{PEV} \tag{38}$$

$$\underline{f_3} = f_3^{(2.1)} \rightarrow \underset{\boldsymbol{x}, \varepsilon_0^{PEV}}{\operatorname{argmin}} f_3\left(\mathrm{E}(\Theta)\right) \tag{39}$$

s.t. (1)-(32) and (38)

$$\underline{\varepsilon}^{PEV} \leq \varepsilon_0^{PEV} \leq \mathrm{E}(\varepsilon_0^{PEV}) \tag{40}$$

To minimize the PEV time window, additional constraints and variables must be declared. Firstly, the constraint (11) is replaced by (41), in which an additional binary variable z_t^{PEV} has been included. This variable will be equal to 1 when the PEV is parked at home and 0 otherwise, this way, it is used to indirectly model the time set Θ, as expressed by equation (42).

$$p_{r|t}^{PEV,i} \leq z_t^{PEV} \cdot u_{r|t}^{PEV,i} \cdot \bar{p}^{PEV};\ \forall r \in \mathcal{R} \wedge t \in \mathcal{T} \wedge i \in \{ch, dch\} \tag{41}$$

$$\Theta = \left\{\boldsymbol{z}^{PEV} \in \mathbb{B}^{\mathrm{size}(\mathcal{T})}: z_t^{PEV} = 1\right\};\ \boldsymbol{z}^{PEV} = \left[z_1^{PEV}, z_2^{PEV}, \dots, z_{\mathcal{T}(\mathrm{end})}^{PEV}\right] \tag{42}$$

It is important to note that the inclusion of z_t^{PEV} in (41) provokes nonlinearity, nevertheless, it can be easily linearized by imposing additional constraints and variables (see Appendix A). For simplicity, it is assumed that the PEV leaves and arrive in the home once over the time horizon, which implies continuity of the vector $\boldsymbol{z}^{PEV}$. To properly model this behaviour, two binary variables namely $arrive_t^{PEV}$ and $departure_t^{PEV}$ are declared, which are equal to 1 if the PEV arrives or leaves the home at the t^{th} time step, respectively, and 0 otherwise. These auxiliary variables allow to include the constraints (43) and (44), which impose continuity in $\boldsymbol{z}^{PEV}$.

$$arrive_t^{PEV} - departure_t^{PEV} = z_t^{PEV} - z_{t-1}^{PEV};\ \forall r \in \mathcal{R} \wedge t \in \mathcal{T} \backslash t \\ > 1 \tag{43}$$

$$\sum_{t \in \mathcal{T}} \{arrive_t\} = 1, \sum_{t \in \mathcal{T}} \{departure_t\} = 1 \tag{44}$$

Thereby, it can be calculated the earliest hour at which the PEV could leave the home, which is equivalent to finding the minimum size of the window Θ, leading to the following optimization problem.

$$f_4 = \sum_{t \in \mathcal{T}} \{\boldsymbol{z}^{PEV}\} \tag{45}$$

$$\underline{f_4} = f_4^{(2.2)} \rightarrow \underset{\boldsymbol{x},\boldsymbol{z}^{PEV}}{\operatorname{argmin}} f_4\left(\mathrm{E}(\varepsilon_0^{PEV})\right) \tag{46}$$

s.t. (1)-(10), (12)-(32), (41)-(44)

4.4 - Stage 3

The Stage 3 is focused on finding a compromise solution among objectives, while immunity against the PEV-related uncertainties is kept. For that purpose, the IGDT has been considered. This approach allows finding robust solutions by taking into account worst-case values of uncertainties. This way, it is not necessary any knowledge of the probability functions of such uncertainties [47], which supposes an advantage in the case of electric vehicles, whose behaviour is highly unpredictable [43].

The IGDT procedure is therefore focused on finding the maximum value of the so-called uncertain radiuses α's. These parameters model the deviation of uncertainty concerning on its expected value. This way, the solution is more robust-oriented whether higher radiuses are obtained. To find the extreme values of the uncertainties related to the PEV, both the initial SOC and PEV time window have to be treated as variables, as explained in Section 4.3. On the other hand, their respective radiuses have to be also included as variables, allowing the uncertainties to vary from their minimum values calculated at the Stage 2, to their expected values, as follows

$$f_3^{(3)} \leq \mathrm{E}(\varepsilon_0^{PEV}) - \alpha_3 \cdot \left(\mathrm{E}(\varepsilon_0^{PEV}) - \underline{f_3}\right) \tag{47}$$

$$f_4^{(3)} \leq \mathrm{E}(\Theta) - \alpha_4 \cdot \left(\mathrm{E}(\Theta) - \underline{f_4}\right) \tag{48}$$

Nevertheless, the objective of the Stage 3 is in fact twofold, since, along with the maximum value of the uncertain radiuses, the compromise solution among objectives have to be found. Accordingly, both concerned objectives are modelled as 'artificial uncertainties' being so possible including them within the IGDT procedure. This novel

paradigm assumes that both the energy cost and consumed net energy can vary from minimum and maximum values, as mentioned in equation (49).

$$f_i^{(3)} \leq \overline{f}_i - \alpha_i \cdot \left(\overline{f}_i - \underline{f_i}\right); i = 1,2 \tag{49}$$

where the minimum values are already calculated at the Stage 1 and the maximum ones can be found as follows.

$$\overline{f}_1 = \max\left(f_1^{(1.2)}, f_1^{(2.1)}, f_1^{(2.2)}\right) \tag{50}$$

$$\overline{f}_2 = \max\left(f_2^{(1.1)}, f_2^{(2.1)}, f_2^{(2.2)}\right) \tag{51}$$

It is worth observing that the higher value of the radiuses related to the objective functions implies the lower value of such functions. Thus, the objective of the Stage 3 is reduced to find the maximum values of all the radiuses α's, which is equivalent to minimizing the value of the objective functions while the degree of robustness against the PEV-related uncertainties is increased at once, as stated in the following optimization problem.

$$\max_{\boldsymbol{x},\varepsilon_0^{PEV},\boldsymbol{z}^{PEV},\boldsymbol{\alpha}} \left[\frac{1}{\text{size}(\boldsymbol{\alpha})} \cdot \sum\{\boldsymbol{\alpha}\};\ \boldsymbol{\alpha}\right] = [\alpha_1, \alpha_2, \alpha_3, \alpha_4] \tag{52}$$

s.t. (1)-(10), (12)-(32), (40)-(44), (47)-(49)

It is noteworthy that the model developed in this paper forces the radiuses to vary from 0 to 1, thus allowing to consider all of them in the same objective function easily [31]. The developed formulation is a MILP (including the linearization techniques in Appendix A), being easily solvable by standard solvers. In addition, its computational complexity grows polynomial with the variable-space size [49].

5 - Case study

In this section, the developed solution procedure is tested and validated, for which a benchmark home installation is profusely studied. The developed optimization problem is coded in Matlab R2019a and solved using Gurobi [50]. The scheduling problem has

been solved over a 24-h time horizon, with 30-min resolution ($\Delta\tau = 0.5$ h). The experiments carried out by the authors on an Intel® Core™ i7-10700K (32 GB RAM) revealed good computational performance, consuming 5 minutes on average to complete the whole procedure, which is considered acceptable and competitive for HEM-related tools [25].

5.1 - Data

It is assumed that the maximum power that can be purchased from the utility grid is 10 kW. The nZEB system under study encompasses two renewable generators and a BES. As described in Section 2, a small-scale PV array and WG are deployed together with a Li-ion battery bank, whose relevant data are extracted from [11, 37] and collected in Table 2. The thermal data is taken from [10], assuming rectangular geometry of the building, while the parameters of the HVAC system and EWH are extracted from [10, 44], and collected in Tables 3 and 4.

Table 2 - Data of renewable generators and BES [11, 37]

Parameter	Value
$\overline{p}^{PV}/\overline{p}^{WT}/\overline{p}^{BES}$	1/1/1.25 kW
$\eta^{PV}/\eta^{WT}/\eta^{BES}$	0.167/0.485/0.98 pu
$\underline{\gamma}^{WT}/\gamma^{WT,*}/\overline{\gamma}^{WT}$	2, 11, 21 m/s
a/b	0.0756 kW/(m/s)³/0.006
$\bar{\varepsilon}^{BES}/\underline{\varepsilon}^{BES}$	5/2 kWh

Table 3 - Data of the HVAC system [10]

Parameter	Value
$\overline{p}^{HVAC}$	2 kW
C^{HVAC}	1.2
$\theta^{HVAC,sp/db}$	23/0.5 ºC

Table 4 - Data of the EWH [44]

Parameter	Value
$\overline{p}^{EWH}$	2.1 kW
η^{EWH}	0.9 pu
$\overline{v}^{EWH}$	50 gal
$R^{w,h}$	863.4 ºC/kWh
$C^{w,h}$	1.52 ºC/kW
$\underline{\theta}^{EWH}/\overline{\theta}^{EWH}/\theta^{w,c}$	45/60/10 ºC

Table 5 - Characteristics of the controllable appliances [21]

Appliance	Power (kW)	φ (hrs.)	Ψ	Type
Dishwasher	2.5	2	1:00-18:00	Interruptible
Washing machine	3	3	1:00-12:00	Non-interruptible
Spin dryer	2.5	1	13:00-21:00	Interruptible

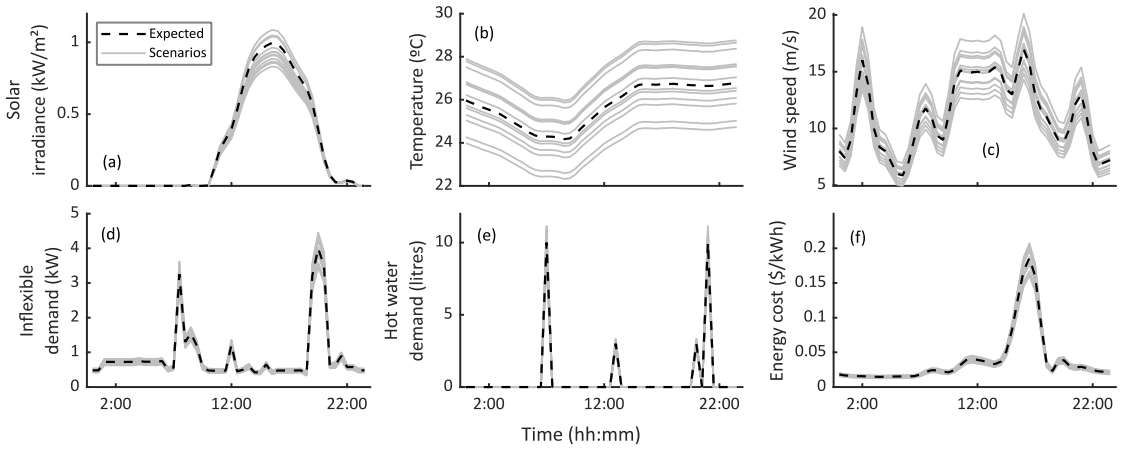

Figure 5 - Expected profiles (discontinuous black line) and representative scenarios (grey solid lines) solar irradiance (a), outdoor temperature (b), wind speed (c), inflexible demand (d), hot water demand (e) and energy price (f)

A Hyundai IONIQ is considered as a benchmark PEV. This vehicle has an on-board 38.3 kWh Li-ion battery system, whose efficiency is taken equal to 0.98 pu [51]. It is assumed that the on-board batteries can be discharged up to 20% of their total capacity. The expected initial SOC for the PEV is 60% of its nominal capacity, while its departure is expected to take place at 9:30 h. The PEV is connected to the home through a 7 kW bidirectional charger.

The HEM system can schedule the operation of the dishwasher, washing machine and spin dryer, whose characteristics are adapted from [21] and collected in Table 5. As seen, the predefined time windows contemplate priority in appliances operation. This way, the dryer cannot be scheduled until the washing machine has not completed its duty cycle. Various real profiles are considered for the stochastic parameters, which are plotted in Fig. 5. The solar irradiance, temperature and wind speed were measured at Virgin Islands on May 3, 2016 [52]. The instantaneous demand attributable to non-controllable

appliances and hot water demand are taken from [11], while the energy pricing on the PJM FE Ohio on July 9, 2019 [53] is taken as RTP purchasing price for the home system under study. After performing the stochastic modelling described in Section 4.1, a total of thirteen representative scenarios are considered in simulations, which are also plotted in Fig. 5.

5.2 - Results and discussion

Herein, various results are provided with a twofold objective. On the one hand, we aim to validate the developed model while on the other hand the effect of PEV-related uncertainties is drawn. Firstly, various simulations are performed observing the effect of various parameters on the outputs of the problem. In this regard, some parameters are freely taken and parametric analyses are carried out. Fig. 6 shows the total energy cost for various capacities of the BES. In this figure, the energy cost is shown at two different stages, namely 1.1 and 3. In the former, the electricity bill is minimized while in the latter a compromise solution among objectives is found taken into account the effect of PEV uncertainties using IGDT. As observed, the economy of the system improves with the size of the batteries, which is logical and coherent since the BES allows a more efficient energy use. The energy cost is notably higher at Stage 3, since in this case the secondary objectives and immunity against PEV uncertainties are improved at expenses of the economy of the installation.

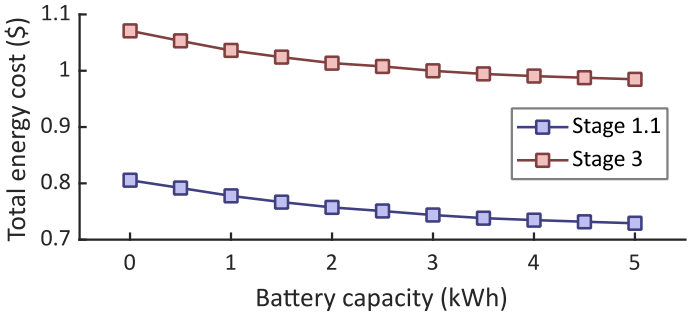

Figure 6 - Total energy cost for various BES sizes

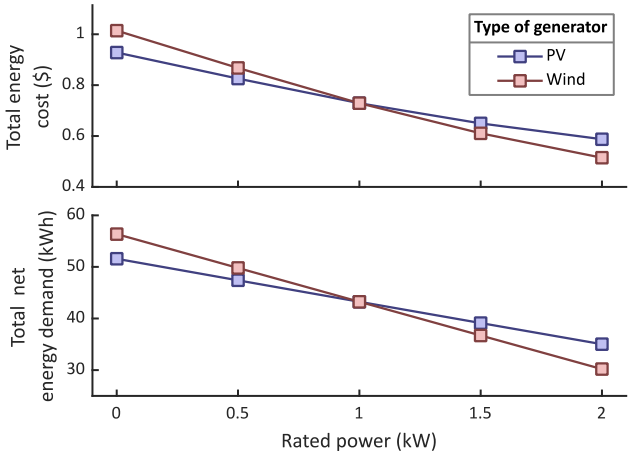

Figure 7 - Total energy cost (upper) and net energy demand (lower) for various sizes of the renewable generators

Table 6 - Results obtained with the developed methodology

Function	Stage 1.1	Stage 1.2	Stage 2.1	Stage 2.2	Stage 3
f_1 ($)	0.729	1.136	1.937	1.704	0.985
f_2 (kWh)	43.97	43.24	81.69	65.35	59.21
f_3 (%)	60	60	20	60	20
f_4 (time slots)	20 (9:30 h)	20 (9:30 h)	20 (9:30 h)	5 (2:30 h)	9 (4:30 h)

A similar simulation is performed for various RES sizes, whose results are plotted in Fig. 7. Obviously, both the energy cost and net energy demand decreases with the rated renewable capacity. It is noteworthy that both indicators are more sensitive to the WG rated power than PV, which is reasonable because wind resource is more available throughout the day than solar irradiation.

The developed procedure is then performed considering the maximum rated capacity of RESs and BES showed in Figs. 1 and 2. Our method calculates a compromise solution among objectives. In this way, the results yielded at Stage 3 should be between the Utopia (minimum) and pseudo-Nadir (maximum) values of each objective [25]. Table 6 reports the results obtained through the different stages involved in the developed procedure. As observed, the results obtained at Stage 3 meet the requirements of multi-objective optimization, since the different objectives (energy cost and net energy demand) are jointly optimized. Logically, the results obtained at this stage lie between the corresponding minimum and maximum values of each objective, since the solution

calculated implies that one objective cannot be improved without further deteriorating the other. It is worth noting that stages 1.1 and 1.2 effectively optimize their corresponding objectives.

Regarding the PEV-related uncertainties, the results at Stage 2 suppose the worst-case scenario for each uncertainty separately. Indeed, Stage 2 determines that the problem is not feasible whether the initial SOC is lower than 20% or the departure time is earlier than 2:30 h. These results are consistent and rational as the initial SOC cannot be lower than the maximum allowable discharge of the onboard batteries, while they require to be charged at least 2.5 hours at maximum power to be fully charged before leaving the home. At Stage 3, a compromise solution among objectives is found; thus, all the objectives along the uncertainties referred to electric vehicle take values among their extreme points.

These last results can be better appreciated in Fig. 8, where the SOC of the PEV is plotted for different stages. As seen, Stage 1.1 considers expected values for the initial SOC and departure times. In contrast, the initial SOC is equal to 20% at Stage 2.1 while the departure takes place at 2:00 h in Stage 2.2. Lastly, Stage 3 finds a compromise solution among objectives, delaying the departure time to 2:30 h but considering the minimum initial SOC.

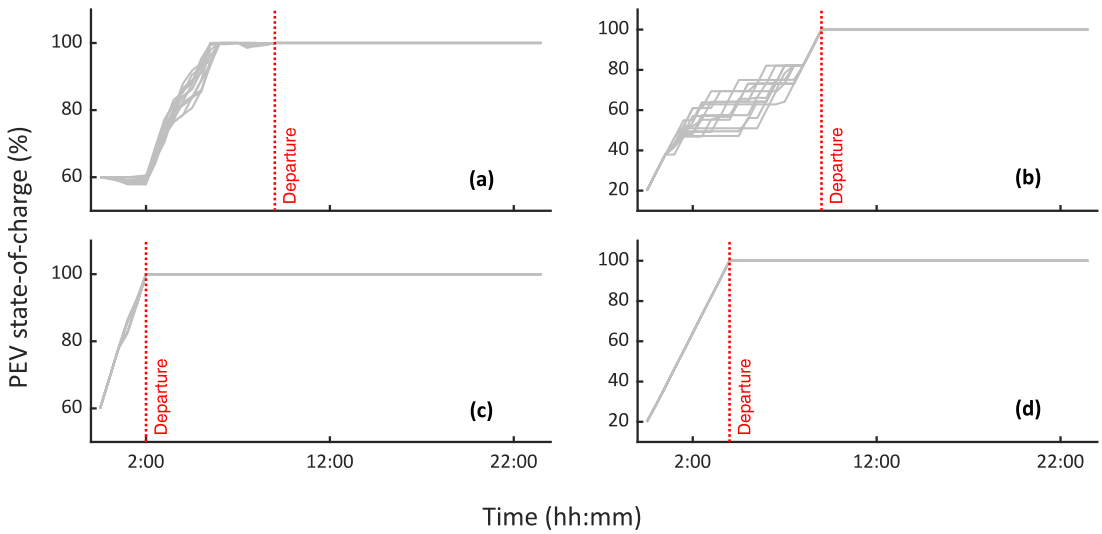

Figure 8 - SOC of the PEV at Stage 1.1 (a), Stage 2.1 (b), Stage 2.2 (c) and Stage 3 (d)

It is worth noting that the V2H capability of the PEV cannot be exploited when its uncertainties are considered. Also, the on-board batteries are only scheduled in discharging mode at Stage 1.1, thus complementing stationary batteries incrementing the storage capacity of the installation. Moreover, V2H can be used instead of stationary batteries in smart homes to avoid the investment necessary to purchase such devices. Fig. 9 plots the scheduling result at different stages of the developed procedure. As illustrated in this figure, when PEV-related uncertainties are neglected, the V2H capability can be slightly exploited, especially during dawn when the PEV replaces the role of the BES. In contrast, considering the worst-case scenario of uncertainties hinders the possibility of exploiting V2H as the vehicle has to be rapidly charged before departure.

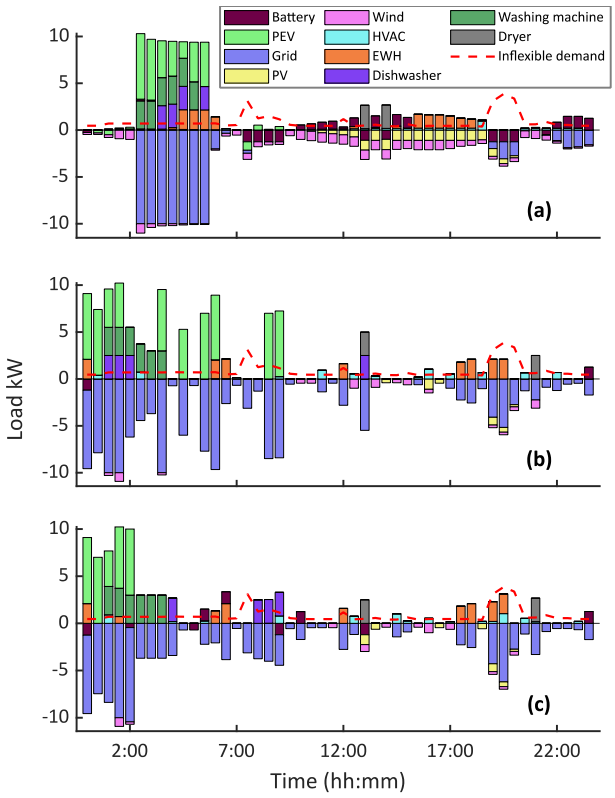

Figure 9 - Scheduling result at Stage 1.1 (a), Stage 2.1 (b) and Stage 2.2 (c)

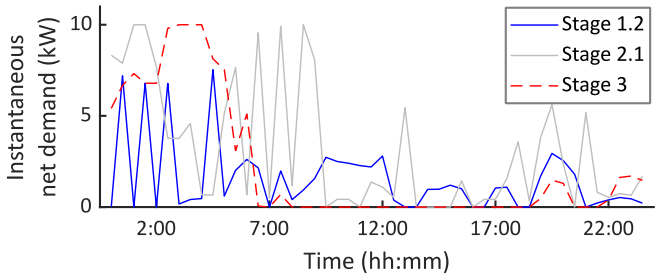

Figure 10 - Instantaneous net demand at different stages

Lastly, the effect of PEV-related uncertainties on the instantaneous net demand is analysed. As revealed in Fig 10, where the instantaneous net demand for different cases is plotted, when the uncertainties are considered, high peak power is shifted from early morning to dawn. This is because the PEV demands high power to be charged before leaving the house. At Stage 2.1, it is assumed that the initial SOC is equal to 20%, which supposes an extreme value (see Fig. 10). In such circumstances, the PEV demands much more energy from the grid (30.4 kWh in total), importing its rated power frequently. The same pattern is observed at Stage 3, since the initial SOC is also equal to 20%. However, at Stage 1.2 the peak power is notably reduced. At this stage, the net energy demand is minimized and expected values for the uncertainties referred to the vehicle take expected values, which supposes a much more favourable scenario.

6 - Conclusions

In this paper, a novel methodology for Home Energy Management in nearly-Zero Energy Buildings under various uncertainties circumstances has been developed. The proposed methodology tackles two main issues of this kind of problems. On the one hand, various objectives are jointly optimized employing a lexicographic-based optimization framework. On the other hand, a hybrid stochastic-IGDT approach has been developed to manage the conventional uncertainties (demand, energy price and weather parameters) as well as the uncertainties brought by V2H facilities. Other advantages referred to

computational tractability and modularity of the proposed procedure have been highlighted, thus proving the usefulness of the developed tool.

The proposed methodology has been tested on a benchmark nZEB system, encompassing solar and wind-based generators, controllable appliances, PEV, thermostatically-controlled loads and storage facilities. To validate the new methodology, energy cost and net energy demand have been taken as objectives. The obtained results prove the effectiveness of the developed methodology to deal with multi-objective optimization, attaining compromise solutions among different objectives. In addition, it has been illustrated how the developed procedure is able to find the worst-case scenario for the uncertainties referred to the PEV using IGDT. In this sense, these extreme cases have been identified at minimum initial SOC of 20% and only 2 h plugged hours. By translating these results into the multi-objective paradigm, the objectives can be treated as artificial uncertainties using the proposed novel IGDT-based approach. The result calculated at third stage considers an initial SOC of 20% (worst-case) while the total available hours for PEV scheduling were 4.5 hours (5 hours less than the expected). In this way, the multi-objective result calculated is also immune against the PEV-related uncertainties.

The developed paradigm could be adapted to other similar systems with high renewable penetration like microgrids. Moreover, the developed formulation could be easily adapted to design stages, thus developing novel planning tools. These issues will be studied in future works.

Appendix A - Linearization of bi-integer terms

Bi-linear terms introduce nonlinearities that may be problematic to solve using standard solvers. Nevertheless, they can be easily linearized by introducing additional

variables and constraints. Let y_1 and y_2 be integer variables. So, their product can be replaced by the linear variable ω introducing the following constraints [42].

$$\omega \leq y_1, \omega \leq y_2 \tag{A1}$$

$$\omega \geq y_1 + y_2 - 1 \tag{A2}$$

$$\omega \geq 0 \tag{A3}$$

Acknowledgements

The icons used through this paper were developed by Freepik, AmethystDesign, Arkinasi and Smashicons from www.flaticon.com.

References

[1] International Energy Agency. World Energy Outlook 2021. Online, available at: https://www.iea.org/reports/world-energy-outlook-2021, (accessed Nov. 21, 2021).

[2] European Commission. Green paper - A 2030 framework for climate and energy policies. Brussels (Belgium), March 27, 2013 (169 final). Online, available at: https://eur-lex.europa.eu/LexUriServ/LexUriServ.do?uri=COM:2013:0169:FIN:en:PDF, (accessed Nov. 21, 2021).

[3] D. D'Agostino, L. Mazzarella. What is a Nearly zero energy building? Overview, implementation and comparison of definitions. *Journal of Building Engineering* 2019; 21: 200-12. https://doi.org/10.1016/j.jobe.2018.10.019.

[4] European Commission. Directive 2018/844/EU 2010 European Parliament and of the Council of 30 May 2018 amending Directive 2010/31/EU on the energy performance of buildings and Directive 2012/27/EU on energy efficiency. 2018.

[5] European Commission. Commission Recommendation (EU) 2016/1318 of 29 July 2016 on guidelines for the promotion of nearly zero-energy buildings and best practices to ensure that, by 2020, all new buildings are nearly zero-energy buildings. 2016.

[6] A.E. Nezhad, A. Rahimnejad, S.A. Gadsden. Home energy management system for smart buildings with inverter-based air conditioning system. *International Journal of Electrical Power & Energy Systems* 2021; 133: 107230. https://doi.org/10.1016/j.ijepes.2021.107230.

[7] U.S. Department of Energy. Quadrennial Technology Review: An Assessment of Energy Technologies and Research Opportunities 2015. Online, available at: https://www.energy.gov/quadrennial-technology-review-2015, (accessed Oct. 24, 2021).

[8] T. Kern, P. Dossow, E. Morlock. Revenue opportunities by integrating combined vehicle-to-home and vehicle-to-grid applications in smart homes. *Applied Energy* 2021; In press: 118187. https://doi.org/10.1016/j.apenergy.2021.118187.

[9] M. Tostado-Véliz, S. Mouassa, F. Jurado. A MILP framework for electricity tariff-choosing decision process in smart homes considering 'Happy Hours' tariffs. *International Journal of Electrical Power & Energy Systems* 2021; 131: 107139. https://doi.org/10.1016/j.ijepes.2021.107139.

[10] N.G. Paterakis, O. Erdinç, A.G. Bakirtzis, J.P.S. Catalão. Optimal Household Appliances Scheduling Under Day-Ahead Pricing and Load-Shaping Demand Response Strategies. *IEEE Transactions on Industrial Informatics* 2015; 11(6): 1509-19. https://doi.org/10.1109/TII.2015.2438534.

[11] M. Tostado-Véliz, R.S. León-Japa, F. Jurado. Optimal electrification of off-grid smart homes considering flexible demand and vehicle-to-home capabilities. *Applied Energy* 2021; 298: 117184. https://doi.org/10.1016/j.apenergy.2021.117184.

[12] H. Kazmi, S. D'Oca, C. Delmastro, S. Lodeweyckx, S.P. Corgnati. Generalizable occupant-driven optimization model for domestic hot water production in NZEB. *Applied Energy* 2016; 175: 1-15. https://doi.org/10.1016/j.apenergy.2016.04.108.

[13] H.J. Kang. Development of an Nearly Zero Emission Building (nZEB) Life Cycle Cost Assessment Tool for Fast Decision Making in the Early Design Phase. *Energies* 2017; 10: 59. https://doi.org/10.3390/en10010059.

[14] N. Javaid, et al. Demand Side Management in Nearly Zero Energy Buildings Using Heuristic Optimizations. *Energies* 2017; 10: 1131. https://doi.org/10.3390/en10081131.

[15] F. Luo, G. Ranzi, W. Kong, Z.Y. Dong, F. Wang. Coordinated residential energy resource scheduling with vehicle-to-home and high photovoltaic penetrations. *IET Renewable Power Generation* 2018; 12(6): 625-32. https://doi.org/10.1049/iet-rpg.2017.0485.

[16] M. Shafie-Khah, P. Siano. A Stochastic Home Energy Management System Considering Satisfaction Cost and Response Fatigue. *IEEE Transactions on Industrial Informatics* 2018; 14(2): 629-38. https://doi.org/10.1109/TII.2017.2728803.

[17] P. Zhao, H. Wu, C. Gu, I. Hernando-Gil. Optimal home energy management under hybrid photovoltaic-storage uncertainty: a distributionally robust chance-constrained approach. *IET Renewable Power Generation* 2019; 13(11): 1911-19. https://doi.org/10.1049/iet-rpg.2018.6169.

[18] C. Abreu, et al. Application of Genetic Algorithms and the Cross-Entropy Method in Practical Home Energy Management Systems. *IET Renewable Power Generation* 2019; 13(9): 1474-83. https://doi.org/10.1049/iet-rpg.2018.6022.

[19] D. Heim, M. Pawlowski. The Methodology of Thermal Energy Management for Nearly Zero Energy Buildings. *Periodica Polytechnica Civil Engineering* 2019; 63(2): 499-517. https://doi.org/10.3311/PPci.12973.

[20] A. O'Donovan, P.D. O'Sullivan, M.D. Murphy. Predicting air temperatures in a naturally ventilated nearly zero energy building: Calibration, validation, analysis and approaches. *Applied Energy* 2019; 250: 991-1010. https://doi.org/10.1016/j.apenergy.2019.04.082.

[21] M.S. Javadi, et al. Optimal Self-scheduling of Home Energy Management System in the Presence of Photovoltaic Power Generation and Batteries. *Energy* 2020; 210: 118568. https://doi.org/10.1016/j.energy.2020.118568.

[22] E. Tsioumas, N. Jabbour, M. Koseoglou, C. Mademlis. A Novel Control Strategy for Improving the Performance of a Nearly Zero Energy Building. *IEEE Transactions on Power Electronics* 2020; 35(2): 1513-24. https://doi.org/10.1109/TPEL.2019.2921107.

[23] G.S. Georgiou, P. Nikolaidis, S.A. Kalogirou, P. Christodoulides. A Hybrid Optimization Approach for Autonomy Enhancement of Nearly-Zero-Energy Buildings Based on Battery Performance and Artificial Neural Networks. *Energies* 2020; 13: 3680. https://doi.org/10.3390/en13143680.

[24] G.S. Georgiou, P. Nikolaidis, S.A. Kalogirou. Optimizing the energy storage schedule of a battery in a PV grid-connected nZEB using linear programming. *Energy* 2020; 208: 118177. https://doi.org/10.1016/j.energy.2020.118177.

[25] M.S. Javadi, et al. Self-scheduling model for home energy management systems considering the end-users discomfort index within price-based demand response programs. *Sustainable Cities and Society* 2021; 68: 102792. https://doi.org/10.1016/j.scs.2021.102792.

[26] G. Mancò, E. Guelpa, A. Colangelo, A. Virtuani, T. Morbiato, V. Verda. Innovative Renewable Technology Integration for Nearly Zero-Energy Buildings within the Re-COGNITION Project. *Sustainability* 2021; 13: 1938. https://doi.org/10.3390/su13041938.

[27] E. Tsioumas, N. Jabbour, M. Koseoglou, D. Papagiannis, C. Mademlis. Enhanced Sizing Methodology for the Renewable Energy Sources and the Battery Storage System in a Nearly Zero Energy Building. *IEEE Transactions on Power Electronics* 2021; 36(9): 10142-56. https://doi.org/10.1109/TPEL.2021.3058395.

[28] R. Ahmadiahangar, et al. Analytical approach for maximizing self-consumption of nearly zero energy buildings- case study: Baltic region. *Energy* 2022; 238: 121744. https://doi.org/10.1016/j.energy.2021.121744.

[29] A. Ghasempour. Advanced Metering Infrastructure in Smart Grid: Requirements, Challenges, Architectures, technologies, and Optimizations. in *Smart Grids: Emerging Technologies, Challenges and Future Directions* 2017; Nova Science Publishers, Hauppauge, NY: 77-127.

[30] M. Tostado-Véliz, S. Gurung, F. Jurado. Efficient solution of many-objective Home Energy Management systems. *International Journal of Electrical Power & Energy Systems* 2022; 136: 107666. https://doi.org/10.1016/j.ijepes.2021.107666.

[31] G. Hernández-Rodríguez. Multiobjective optimization of natural gas transportation networks. PhD thesis; 2011. Institut National Polytechnique de Toulouse. Available at: https://oatao.univ-toulouse.fr/7129/1/hernandez_rodriguez.pdf, (accessed Oct. 23, 2021).

[32] M. Nazari-Heris, et al. A hybrid robust-stochastic optimization framework for optimal energy management of electric vehicles parking lots. *Sustainable Cities & Society* 2021; 47: 101467. https://doi.org/10.1016/j.seta.2021.101467.

[33] M. Vahid-Ghavidel, et al. Novel Hybrid Stochastic-Robust Optimal Trading Strategy for a Demand Response Aggregator in the Wholesale Electricity Market. *IEEE Transactions on Industry Applications* 2021; 57(5): 5488-98. https://doi.org/10.1109/TIA.2021.3098500.

[34] H. Rashidizadeh-Kermani, M. Vahedipour-Dahraie, A. Anvari-Moghaddam, J.M. Guerrero. A stochastic bi-level decision-making framework for a load-serving entity in day-ahead and balancing markets. *International Transactions on Electrical Energy Systems* 2019; 29(11): e12109. https://doi.org/10.1002/2050-7038.12109.

[35] I.K. Bazionis, P.A. Karafotis, P.S. Georgilakis. A review of short-term wind power probabilistic forecasting and a taxonomy focused on input data. *IET Renewable Power Generation* 2021. https://doi.org/10.1049/rpg2.12330.

[36] H. Khaloie, et al. Offering and bidding for a wind producer paired with battery and CAES units considering battery degradation. *International Journal of Electrical Power & Energy Systems* 2022; 136: 107685. https://doi.org/10.1016/j.ijepes.2021.107685.

[37] M. Tostado-Véliz, P. Arévalo, F. Jurado. A comprehensive electrical-gas-hydrogen Microgrid model for energy management applications. *Energy Conversion & Management* 2021; 228: 113726. https://doi.org/10.1016/j.enconman.2020.113726.

[38] S. Mandal, B.K. Das, N. Hoque. Optimum sizing of a stand-alone hybrid energy system for rural electrification in Bangladesh. *Journal of Cleaner Production* 2018; 200: 12-27. https://doi.org/10.1016/j.jclepro.2018.07.257.

[39] M. Tostado-Véliz, M. Bayat, A.A. Ghadimi, F. Jurado. Home energy management in off-grid dwellings: Exploiting flexibility of thermostatically controlled appliances. *Journal of Cleaner Production* 2021; 310: 127507. https://doi.org/10.1016/j.jclepro.2021.127507.

[40] A. Ali, K. Mahmoud, M. Lehtonen. Enhancing hosting capacity of intermittent wind turbine systems using bi-level optimisation considering OLTC and electric vehicle charging stations. *IET Renewable Power Generation* 2020; 14(17): 3558-67. https://doi.org/10.1049/iet-rpg.2020.0837.

[41] P. Arévalo, M. Tostado-Véliz, F. Jurado. A Novel Methodology for Comprehensive Planning of Battery Storage Systems. *Journal of Energy Storage* 2021; 37: 102456. https://doi.org/10.1016/j.est.2021.102456.

[42] M. Tostado-Véliz, S. Kamel, F. Aymen, A.R. Jordehi, F. Jurado. A Stochastic-IGDT model for energy management in isolated microgrids considering failures and demand response. *Applied Energy* 2022; 317: 119162. https://doi.org/10.1016/j.apenergy.2022.119162.

[43] G.J. Osório, et al. Modeling an electric vehicle parking lot with solar rooftop participating in the reserve market and in ancillary services provision. *Journal of Cleaner Production* 2021; 318: 128503. https://doi.org/10.1016/j.jclepro.2021.128503.

[44] P. Du, N. Lu. Appliance Commitment for Household Load Scheduling. *IEEE Transactions on Smart Grid* 2011; 2(2): 411-9. https://doi.org/10.1109/TSG.2011.2140344.

[45] M. Mansour-Lakouraj, H. Niaz, J.J. Liu, P. Siano, A. Anvari-Moghaddam. Optimal risk-constrained stochastic scheduling of microgrids with hydrogen vehicles in real-time and day-ahead markets. *Journal of Cleaner Production* 2021; 318: 128452. https://doi.org/10.1016/j.jclepro.2021.128452.

[46] J.S. Arora. *Introduction to Optimum Design*, 4th ed. Cambridge, MA: Academic Press; 2017. https://doi.org/10.1016/C2013-0-15344-5.

[47] M. Ahrabi, et al. Evaluating the effect of electric vehicle parking lots in transmission-constrained AC unit commitment under a hybrid IGDT-stochastic approach. *International Journal of Electrical Power & Energy Systems* 2021; 125: 106546. https://doi.org/10.1016/j.ijepes.2020.106546.

[48] M. Tostado-Véliz, D. Icaza-Álvarez, F. Jurado. A novel methodology for optimal sizing photovoltaic-battery systems in smart homes considering grid outages and demand response. *Renewable Energy* 2021; 170: 884-96. https://doi.org/10.1016/j.renene.2021.02.006.

[49] I.A. Avramidis, F. Capitanescu, G. Deconinck. A generic multi-period optimal power flow framework for combating operational constraints via residential flexibility resources. *IET Generation, Transmission & Distribution* 2021; 15(2): 306-20. https://doi.org/10.1049/gtd2.12022.

[50] Gurobi Optimization L.L.C. Gurobi Optimizer Reference Manual, 2021. Online, available at: https://www.gurobi.com, (accessed Nov. 29, 2021)

[51] I. Alsaidan, A. Khodaei, W. Gao. A Comprehensive Battery Energy Storage Optimal Sizing Model for Microgrid Applications. *IEEE Transactions on Power Systems* 2018; 33(4): 3968-80. https://doi.org/10.1109/TPWRS.2017.2769639.

[52] NOAA. Land base datasets. Online, available at: https://www.ncdc.noaa.gov/data-access/land-based-station-data/land-based-datasets, (accessed Nov. 29, 2021).

[53] Engie. Historical data reports. Online, available at: https://www.engieresources.com/historical-data#reports_anchor, (accessed Nov. 29, 2021).